CRN 96–01
TK 96 02
hep-ph/9601nnn

IMPROVED DESCRIPTION OF THRESHOLD PION ELECTROPRODUCTION IN CHIRAL PERTURBATION THEORY

V. Bernard [a 1], N. Kaiser [b 2], Ulf-G. Meißner [c 3]

[a] *Laboratoire de Physique Théorique, Institut de Physique*
3-5 rue de l'Université, F-67084 Strasbourg Cedex, France
Centre de Recherches Nucléaires, Physique Théorique
BP 28, F-67037 Strasbourg Cedex 2, France

[b] *Technische Universität München, Physik Department T39*
James-Franck-Straße, D-85747 Garching, Germany

[c] *Institut für Theoretische Kernphysik, Universität Bonn*
Nußallee 14–16, D-53115 Bonn, Germany

Abstract

We investigate neutral pion electroproduction off protons in the framework of heavy baryon chiral perturbation theory. The chiral expansion of the S–wave multipoles E_{0+} and L_{0+} is carried out to three orders. There appear several undetermined low–energy constants. Three are taken from a recent study of the new TAPS threshold π^0 photoproduction data, one is fixed from the proton Dirac form factor and the novel S–wave constants appearing at orders q^4 and q^5 are determined from a best fit (constrained by resonance exchange) to the recent NIKHEF and MAMI data at photon momentum transfer squared $k^2 = -0.1$ GeV^2. The inclusion of a particular set of dimension five operators is forced upon the fit by a soft–pion theorem which severely constrains the momentum dependence of the longitudinal S–wave multipole L_{0+} at order q^4. We give predictions for lower photon virtualities for the various multipoles and differential cross sections. Further improvements are briefly touched upon.

[1] email: bernard@crnhp4.in2p3.fr
[2] email: nkaiser@physik.tu-muenchen.de
[3] email: meissner@pythia.itkp.uni-bonn.de

1 Introduction

Chiral perturbation theory (CHPT) allows to systematically investigate the consequences of the spontaneous and the explicit chiral symmetry breaking in QCD. With the advent of CW machines, pion production by real and virtual photons has become a major testing ground for predictions based on nucleon chiral dynamics. In particular, over the last years there has been considerable activity to precisely measure neutral pion electroproduction in the threshold region at various laboratories, in particular at NIKHEF (Amsterdam) and MAMI (Mainz). These measurements are performed at energies very close to threshold and typical photon momentum transfer squared of $k^2 = -0.1$ GeV^2. After the pioneering measurement of Welch et al. [1] at NIKHEF, which concentrated on the S–wave cross section, kinematically more complete differential cross sections for various photon polarizations $\epsilon = 0.5 \ldots 0.9$ are now available based on the data of van den Brink et al. [2] (NIKHEF) and Distler et al. [3] (MAMI). Furthermore, data at lower $|k^2|$ have also been taken at MAMI [4].

In the review [5] we already considered charged and neutral pion electroproduction off protons and neutrons in the framework of relativistic nucleon CHPT [6] to order q^3 (here, q denotes the small expansion parameter which can be an external momentum or meson mass and the order q^n refers to the Lagrangian). Since then, the theoretical framework has been considerably refined based on the heavy mass expansion proposed in [7] and discussed in detail in the recent review [8]. In this framework and calculating the S–waves to order q^4, we have already reexamined neutral pion photoproduction [9,10]. Novel P–wave low–energy theorems (LETs) have been found together with a good description of the new TAPS and SAL data for $\gamma p \to \pi^0 p$ [11] [12]. In particular, chiral loops are necessary to understand the small value of the electric dipole amplitude E_{0+} at the $\pi^0 p$ and $\pi^+ n$ thresholds. Furthermore, the P–wave LETs have been shown to hold within 10% or better. While P_1 can be inferred directly from the unpolarized differential cross section, for P_2 one has to measure polarization observables. A measurement of the photon polarization asymmetry is underway e.g. at MAMI. However, there are somewhat model–dependent means to indirectly determine P_2, see e.g. [13] and [14]. These LET predictions extended to the case of virtual photons [15] were also used in the analysis of the NIKHEF data [2]. The investigation presented here is thus a natural extension of the one for photoproduction presented in [9]. To orders q^3 and q^4, there appear two new counter terms with a priori undetermined low–energy constants (LECs). One can be fixed from a recent dispersion–theoretical fit to the nucleon electromagnetic form factors, i.e. from the radius of the proton Dirac form factor [16]. The other one will be determined from a best fit to the differential cross sections at $k^2 = -0.1$ GeV^2. As we will show, due to a soft–pion theorem, these fits are too constrained since they lead to a k^2–dependence of the longitudinal S–wave multipole L_{0+}

only through Born and one–loop graphs. We therefore are forced to include the leading corrections to this soft–pion theorem in the counter terms which is formally of order q^5 in the Lagrangian. This in turn leads to a satisfactory fit of the existing data at $k^2 = -0.1$ GeV^2 and we then make predictions for smaller values of $|k^2|$, where this dimension five operator is much less important. In addition, three k^2–independent low–energy constants are taken from the photoproduction calculation to order q^4 [10].

The paper is organized as follows. In section 2, we briefly summarize the pertinent kinematics and define the various cross sections and structure functions. We also present the natural basis of S– and P–wave multipoles which appear in the transition matrix–element. In section 3, the chiral expansion of the S–wave multipoles E_{0+} and L_{0+} is given to three orders in small momenta and the five combinations of P–wave multipoles to two orders. The corresponding low–energy theorems were already given in [15]. We also introduce an approximation which facilitates the calculation of the energy–dependence of the S–wave multipoles. In section 4, we give the explicit expression for the various low–energy constants based on the resonance saturation principle. In section 5, the best fits to the differential cross sections are presented together with a detailed analysis of the various multipoles at $k^2 = -0.1$ GeV^2. In section 6, we give predictions for the new data taken at $k^2 = -0.06$ GeV^2 and investigate in some detail the $|k^2|$ range of $0.04 \ldots 0.06$ GeV^2. A short summary together with a discussion of possible improvements is given in section 7. The appendix contains some consideration about the S–wave LECs at order q^4.

2 Formal aspects

In this section, we assemble all the necessary definitions for the cross sections, structure functions and multipoles. To be specific, consider the process

$$\gamma^\star\,(k) + p\,(p_1) \to \pi^0\,(q) + p\,(p_2)\ , \tag{1}$$

where $\gamma^\star$ is the virtual photon with $k^2 < 0$. Denote by W the cm energy of the πN system and its threshold value by $W_0 = M_\pi + m$, with $M_\pi = 134.97$ MeV and $m = 938.27$ MeV the (neutral) pion and the proton mass, respectively. The following quantities are used

$$\begin{aligned} q &= \sqrt{\omega^2 - M_\pi^2}\ , \quad k_0 = \frac{1}{2W}(W^2 - m^2 + k^2)\ , \\ \epsilon^{-1} &= 1 + 2(1 - \frac{k_0^2}{k^2})\,\tan^2\frac{\psi}{2}\ , \quad \epsilon_L = -\frac{k^2}{k_0^2}\,\epsilon\ , \end{aligned}$$

$$\omega = \frac{1}{2W}(W^2 - m^2 + M_\pi^2) \ , \quad \Delta W = W - W_0 \ , \tag{2}$$

with q the pion cm momentum, k_0 the photon energy, ϵ the photon polarization, ϵ_L the longitudinal photon polarization, ψ the electron scattering angle, ω the pion energy in the πN cm system and ΔW gives the invariant energy above threshold. As explained in some detail in [9], we will account for the pion mass difference $M_{\pi^+} - M_{\pi^0}$ in the loops but keeping one nucleon mass. The $\pi^+ n$ threshold is located at $\omega_c = 140.11$ MeV which will also be used as the charged pion mass. We introduce the ratio

$$\rho = -\frac{k^2}{\omega_c^2} > 0 \quad , \tag{3}$$

and as a further dimensionless quantity of order one

$$y = \frac{\omega^2}{\omega_c^2} \quad . \tag{4}$$

y varies between 0.93 and 1.12 for $\Delta W = 0 \ldots 15$ MeV.

The unpolarized pion electroproduction triple differential cross section reads

$$\frac{d\sigma}{dE_f d\Omega_f d\Omega_\pi} = \frac{\alpha E_f (W^2 - m^2)}{4\pi^2 E_i m k^2 (\epsilon - 1)} \frac{d\sigma}{d\Omega_\pi} = \Gamma_V \frac{d\sigma}{d\Omega_\pi} \ , \tag{5}$$

with Γ_V the conventional virtual photon flux factor, $\alpha = e^2/4\pi = 1/137.036$ the fine structure constant and $E_{i/f}$ is the laboratory energy of the incoming/outgoing electron. The differential cross section can be split into transverse (T), longitudinal (L), transverse–longitudinal (TL) and transverse-transverse (TT) terms,

$$\frac{d\sigma}{d\Omega_\pi} = \frac{2Wq}{W^2 - m^2} \Big(R_T + \epsilon_L \, R_L + \sqrt{2\epsilon_L(1+\epsilon)} \cos\phi \, R_{TL} + \epsilon \cos 2\phi \, R_{TT} \Big), \tag{6}$$

where the R_I ($I = T, L, TL, TT$) are called the structure functions. ϕ is the azimuthal angle between the scattering and the reaction plane, and the corresponding polar angle, spanned by the photon and pion directions, is called θ,

$$\cos\theta = \hat{q} \cdot \hat{k} \quad . \tag{7}$$

One also uses the separated virtual photon cross sections

$$\frac{d\sigma_I}{d\Omega_\pi} = \frac{2Wq}{W^2 - m^2}\, R_I, \quad I = T, L, TL, TT \quad . \tag{8}$$

This completes the necessary definitions of kinematical quantities and cross sections.

In what follows, we will consider the threshold region, i.e. small values of ΔW, typically $\Delta W < 15\,\mathrm{MeV}$ and small photon virtualities, $|k^2| \leq 0.1$ GeV^2. In that case, the pion three momentum is small and it is therefore advantageous to perform a multipole decomposition. We confine ourselves to the S– and P–waves in what follows. Consequently, the current matrix element takes the form

$$\begin{aligned}\frac{m}{4\pi W}\,\vec{J} = {} & i\vec{\sigma}\left(E_{0+} + \hat{q}\cdot\hat{k}\,P_1\right) + i\vec{\sigma}\cdot\hat{k}\,\hat{q}\,P_2 + \hat{q}\times\hat{k}\,P_3 \\ & + i\vec{\sigma}\cdot\hat{k}\,\hat{k}\left(L_{0+} - E_{0+} + \hat{q}\cdot\hat{k}\,(P_4 - P_5 - P_1 - P_2)\right) + i\vec{\sigma}\cdot\hat{q}\,\hat{k}\,P_5\,,\end{aligned} \tag{9}$$

in terms of the two S–waves $E_{0+}$and L_{0+} and five P–waves. We choose the following combinations of the more commonly used P–wave multipoles E_{1+}, $M_{1\pm}$ and $L_{1\pm}$, where E, M, L stands for electric, magnetic and longitudinal, respectively and the $\pm$ refers to the total angular momentum of the pion–nucleon system, $j = l \pm 1/2$ (with l the pion angular momentum),

$$\begin{aligned}&P_1 = 3E_{1+} + M_{1+} - M_{1-}, \quad P_2 = 3E_{1+} - M_{1+} + M_{1-}, \\ &P_3 = 2M_{1+} + M_{1-}, \quad P_4 = 4L_{1+} + L_{1-}, \quad P_5 = L_{1-} - 2L_{1+}\ .\end{aligned} \tag{10}$$

These are the combinations which appear naturally in the transition matrix element and lead to the most compact formulae for the various cross sections. All multipoles are, of course, functions of the pion energy and the photon four–momentum squared, like e.g. $E_{0+} = E_{0+}(\omega, k^2)$. In what follows, we will drop these obvious arguments. The structure functions R_I can be expressed in terms of the multipoles as follows (in the S– and P–wave approximation)

$$\begin{aligned}R_T &= |E_{0+} + \cos\theta\, P_1|^2 + \frac{1}{2}\sin^2\theta\,(|P_2|^2 + |P_3|^2)\,, \\ R_L &= |L_{0+} + \cos\theta\, P_4|^2 + \sin^2\theta\,|P_5|^2\,, \\ R_{TL} &= -\sin\theta\,\mathrm{Re}[(E_{0+} + \cos\theta\, P_1)\,P_5^* + (L_{0+} + \cos\theta\, P_4)\,P_2^*]\,, \\ R_{TT} &= \frac{1}{2}\sin^2\theta\,(|P_2|^2 - |P_3|^2)\ .\end{aligned} \tag{11}$$

3 Chiral expansion of the multipoles

To perform the calculations, we make use of the effective Goldstone boson–baryon Lagrangian. Our notation is identical to the one used in [9] and we discuss here only some additional terms. The effective Lagrangian takes the form (to one loop accuracy)

$$\mathcal{L}_{\rm eff} = \mathcal{L}^{(1)}_{\pi N} + \mathcal{L}^{(2)}_{\pi N} + \mathcal{L}^{(3)}_{\pi N} + \mathcal{L}^{(4)}_{\pi N} + \mathcal{L}^{(2)}_{\pi\pi} + \mathcal{L}^{(4)}_{\pi\pi} \tag{12}$$

where the chiral dimension (i) counts the number of derivatives and/or meson mass insertions. We will work out the S–wave multipoles to order q^3 and the P–waves to order q^2 as explained in some detail in ref.[9]. Here, the order refers to the various multipoles. The corresponding Lagrangians are one order higher since the photon polarization vector counts as order q. For the P–waves, we thus have to consider tree graphs with insertions from $\mathcal{L}^{(1,2,3)}_{\pi N}$ and one loop graphs with insertions solely from $\mathcal{L}^{(1)}_{\pi N}$. For the S–wave multipoles, we have in addition to consider one loop diagrams with exactly one insertion from $\mathcal{L}^{(2)}_{\pi N}$ and tree graphs from $\mathcal{L}^{(4)}_{\pi N}$. In comparison to the photoproduction calculation, we have two additional terms with undetermined low-energy constants. One is from $\mathcal{L}^{(3)}_{\pi N}$ and is related to the Dirac form factor of the proton, $F_1^V(k^2)$, and was already considered in the relativistic calculation in [5]. In the heavy fermion approach used here, the effect due to the finite charge radius of the proton manifests itself via

$$< r^2 >^p_1 = \frac{1}{16\pi^2 F_\pi^2}\left[-(5g_A^2+1)\ln\frac{\omega_c}{\lambda} - \frac{7}{2}g_A^2 - \frac{1}{2}\right] + \delta r_{1p}(\lambda) \ , \tag{13}$$

with λ the scale of dimensional regularization, g_A the axial–vector coupling constant and $F_\pi = 93\,\mathrm{MeV}$ the pion decay constant. The terms in the square brackets in Eq.(13) stem from the loops. The constant $\delta r_{1p}(\lambda)$ can be fixed from the recent dispersion–theoretical fit to the nucleon electromagnetic form factors, $< r^2 >^{p,\rm exp}_1 = 0.774 \pm 0.008\,\mathrm{fm}^2$ [16]. The other counter term is from $\mathcal{L}^{(4)}_{\pi N}$ and appears in the chiral expansion of the S–wave multipoles. We do not need the explicit form of this term in the effective Lagrangian in what follows and thus refrain from giving it here. [4]

Consider first the chiral expansion of the P–wave multipoles to order q^3. This should be rather accurate for the large multipoles but is afflicted with some uncertainty for the small ones, compare e.g. the discussion by Bergstrom [13]

[4] As discussed later, we also need to take one particular term from $\mathcal{L}^{(5)}_{\pi N}$ since with the sole k^2–dependent counter term from $\mathcal{L}^{(4)}_{\pi N}$ togther with the radius correction from $\mathcal{L}^{(3)}_{\pi N}$ one is not able to describe the existing data at rather large $|k^2| \simeq 5M_\pi^2$.

for the photoproduction case. He finds a good description of the large multipole $M_{1+} - M_{1-}$ but some sizeable deviation for the much smaller E_{1+}. As we will show later on, the existing electroproduction data are not yet accurate enough to pin down the small multipoles with great precision and we thus stick to the q^3 approximation. [5] The chiral expansion of the P-wave multipoles thus takes the form

$$P_i = P_i^{\rm Born} + P_i^{\rm loop} + P_i^{\rm ct} \ , \quad i = 1, \ldots, 5 \ , \tag{14}$$

with $P_3^{\rm loop} = 0$ and $P_i^{\rm ct} = 0$ for $i = 1, 2, 4, 5$. The Born terms include the contribution from the proton anomalous magnetic moment κ_p, which to lowest order appears in the dimension two pion–nucleon Lagrangian. For the large multipoles $P_{1,2,3}$ we have the following Born (and counter) terms (in case of P_3),

$$P_1^{\rm Born} = \frac{e g_{\pi N}\, q}{8\pi m^2 \omega} \Big\{ (1+\kappa_p)\sqrt{\omega^2 - k^2} + \frac{1}{10 m \omega \sqrt{\omega^2 - k^2}} \times \tag{15}$$
$$[\ 17\omega^2 k^2 - 12\omega^4 + 2\omega^2 M_\pi^2 - 7 k^2 M_\pi^2 + 5\kappa_p (2\omega^2 k^2 - k^2 M_\pi^2 - \omega^4)] \Big\} ,$$

$$P_2^{\rm Born} = \frac{e g_{\pi N}\, q}{8\pi m^2 \omega} \Big\{ -(1+\kappa_p)\sqrt{\omega^2 - k^2} + \frac{1}{10 m \omega \sqrt{\omega^2 - k^2}} \times \tag{16}$$
$$[\ 13\omega^4 - 18\omega^2 k^2 + 2\omega^2 M_\pi^2 + 3 k^2 M_\pi^2 + 5\kappa_p (\omega^4 + k^2 M_\pi^2 - 2\omega^2 k^2)] \Big\} ,$$

$$P_3^{\rm Born+ct} = e\, q \Big(\frac{g_{\pi N}}{16\pi m^3} + b_P \Big) \sqrt{\omega^2 - k^2} \quad , \tag{17}$$

with $g_{\pi N} = 13.4$ the strong pion–nucleon coupling constant. We notice that the P–waves scale with the pion momentum q. The constant b_P has been determined from a best fit to the new TAPS data for $\gamma p \to \pi^0 p$, $b_P = 13.0\,{\rm GeV}^{-3}$, a value which is well understood in terms of Δ and vector meson exchange. However, there are also new data from SAL for the same process. The analysis of these gives a somewhat higher total cross section above $\pi^+ n$ threshold [12]. To account for this, we also use the larger value of $b_P = 15.8\,{\rm GeV}^{-3}$ as determined in [9]. The small multipoles $P_{4,5}$ have the following Born terms

$$P_4^{\rm Born} = \frac{e g_{\pi N}\, q}{40\pi m^3} \Big(2 + 3\frac{M_\pi^2}{\omega^2} \Big) \sqrt{\omega^2 - k^2} \ , \tag{18}$$

$$P_5^{\rm Born} = \frac{e g_{\pi N}\, q}{80\pi m^3} \Big(3 + 2\frac{M_\pi^2}{\omega^2} \Big) \sqrt{\omega^2 - k^2} \ . \tag{19}$$

[5] This should eventually be refined when more accurate data will become available.

All these Born terms are, of course, real. The one loop contribution to the P_i $(i = 1, 2, 4, 5)$ takes the form

$$P_1^{\rm loop} = \frac{e g_{\pi N}^3 \omega_c \, q}{32\pi^2 m^3} \frac{1}{\sqrt{y(y+\rho)^3}} \Big[\frac{\rho}{3} + \frac{3}{8}\rho^2 + \frac{y}{3} + \frac{3}{4}\rho\, y + \frac{y^2}{2} - \sqrt{1-y} \times (\frac{\rho}{3} + \frac{\rho^2}{8} + \frac{y}{3} + \frac{\rho\, y}{6} + \frac{y^2}{6}) - \frac{(\rho+2y)(4\rho+\rho^2+4y)}{16\sqrt{y+\rho}} H(y,\rho) \Big] \ , \quad (20)$$

$$P_2^{\rm loop} = \frac{e g_{\pi N}^3 \omega_c \, q}{32\pi^2 m^3} \frac{1}{\sqrt{y(y+\rho)^3}} \Big[\frac{\rho}{3} - \frac{3}{8}\rho^2 + \frac{y}{3} - \rho\, y - \frac{y^2}{2} + \sqrt{1-y} \times (-\frac{\rho}{3} + \frac{\rho^2}{8} - \frac{y}{3} + \frac{7}{12}\rho\, y + \frac{y^2}{3}) + \frac{\rho(4\rho+\rho^2+4y)}{16\sqrt{y+\rho}} H(y,\rho) \Big] \ , \quad (21)$$

$$P_4^{\rm loop} = \frac{e g_{\pi N}^3 \omega_c \, q}{32\pi^2 m^3} \frac{1}{\sqrt{y(y+\rho)^3}} \Big[\frac{\rho}{3} + \frac{y}{3} - \frac{\rho\, y}{4} - \frac{y^2}{2} + \frac{1}{3}\sqrt{1-y} \times (-\rho - y + \frac{\rho\, y}{4} + y^2) - \frac{(\rho+2y)\rho\, y}{8\sqrt{y+\rho}} H(y,\rho) \Big] \ , \quad (22)$$

$$P_5^{\rm loop} = \frac{e g_{\pi N}^3 \omega_c \, q}{32\pi^2 m^3} \frac{1}{\sqrt{y(y+\rho)^3}} \Big[\frac{\rho}{3} + \frac{y}{3} - \frac{\rho\, y}{8} + \frac{1}{3}\sqrt{1-y} \times (-\rho - y + \frac{5}{8}\rho\, y + \frac{y^2}{4}) - \frac{y(4\rho+\rho^2+4y)}{16\sqrt{y+\rho}} H(y,\rho) \Big] \ , \quad (23)$$

with

$$H(y,\rho) = \arctan \frac{\rho}{2\sqrt{y+\rho}} + \arcsin \frac{\rho+2y}{\sqrt{4\rho+\rho^2+4y}} \ , \quad \omega < \omega_c \ . \quad (24)$$

Loop effects which renormalize physical quantities like e.g. the anomalous magnetic moment κ_p or the pion–nucleon coupling are properly taken care of. For $\omega > \omega_c$, these loop contributions become complex. This has to be accounted for by the substitutions

$$\sqrt{1-y} = -i\sqrt{y-1} \quad , \quad (25)$$

and

$$\arcsin \frac{\rho+2y}{\sqrt{4\rho+\rho^2+4y}} = \frac{\pi}{2} + i \, \ln \frac{\rho+2y+2\sqrt{(y+\rho)(y-1)}}{\sqrt{4\rho+\rho^2+4y}} \ . \quad (26)$$

For the imaginary parts of the P–wave multipoles, one can give a rather compact and accurate description based on the Fermi–Watson final state theorem. This serves as a consistency check and gives a handy and rather accurate

estimate about the size of the Im P_i. Of course, in the full calculations to be performed later, we are not using these approximate forms. Consider the rescattering diagram shown in Fig.1. The corresponding imaginary part can be cast into the product of a charged pion production process followed by a pion–nucleon charge exchange (CEX) reaction. Consequently

$$\mathrm{Im}\,(\mathcal{M})^{\pi^0 p} = q_+^3 \cdot a_{2J}^{\mathrm{CEX}}\ \mathrm{Re}(\mathcal{M})^{\pi^+ n}\ , \tag{27}$$

where $\mathcal{M}$ is a generic symbol for any one of the P–wave multipoles E_{1+}, $M_{1\pm}$, $L_{1\pm}$ and $J = 3/2\ (1/2)$ for the $1+\ (1-)$ multipoles, a_{2J} denotes the corresponding charge–exchange (CEX) scattering volume and $q_+ = \sqrt{\omega^2 - \omega_c^2}$. To lowest order, these scattering volumina are given by

$$a_3^{\mathrm{CEX}} = a_1^{\mathrm{CEX}} = -\frac{\sqrt{2}\, g_A^2}{24\pi M_\pi F_\pi^2}\ . \tag{28}$$

Furthermore, the P–waves for $\gamma p \to \pi^+ n$ can be easily evaluated in Born approximation from the pion pole diagram,

$$\vec{J}^{\,\pi^+ n} = i\frac{e g_A}{\sqrt{2}F_\pi}\vec{\sigma}\cdot(\vec{q}-\vec{k}\,)\,(\vec{k}-2\vec{q}\,)\left[\frac{1}{(2+\rho)M_\pi^2} + \frac{2\vec{q}\cdot\vec{k}}{(2+\rho)^2 M_\pi^4}\right]\ , \tag{29}$$

where the terms in the square brackets come from the expansion of the pion propagator. Evaluating the operator structure of Eq.(29) fixes the $P_i^{\pi^+ n}$. Combining these with CEX scattering volumina and the appropriate kinematical factors, we have

$$\begin{aligned}
&\mathrm{Im}\,P_1^{\pi^0 p} = 0\ ,\ \ \mathrm{Im}\,P_2^{\pi^0 p} = -\frac{e\, g_A^3\, q\, q_+^3}{48\,\pi^2\, F_\pi^3\, M_\pi^2}\frac{\sqrt{1+\rho}}{2+\rho}\ ,\\
&\mathrm{Im}\,P_4^{\pi^0 p} = \frac{4+\rho}{2(2+\rho)}\,\mathrm{Im}\,P_2^{\pi^0 p}\ ,\ \ \mathrm{Im}\,P_5^{\pi^0 p} = \frac{1}{2}\,\mathrm{Im}\,P_2^{\pi^0 p}\ .
\end{aligned} \tag{30}$$

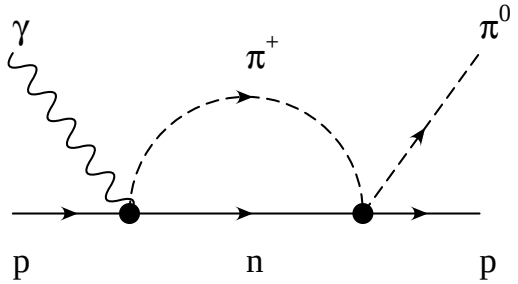

Fig. 1. Rescattering diagram. The solid circles subsume various subdiagrams.

This shows that P_2 has the largest imaginary part. These approximations become very accurate as ρ approaches zero. Isospin breaking effects not taken into account in such a consideration are of the order $(\omega_c^2 - M_{\pi^0}^2)^{3/2}/M_{\pi^0}^3 \sim 2\,\%$.

We now turn to the S–wave multipoles E_{0+} and L_{0+}. Let $\mathcal{S}$ be a generic symbol for either one of them. The chiral expansion carried out to order q^4 takes the form

$$\mathcal{S} = \mathcal{S}^{\rm Born} + \mathcal{S}^{\rm q^3-loop} + \mathcal{S}^{\rm q^4-loop} + \mathcal{S}^{\rm ct} \ . \tag{31}$$

As already mentioned, $\mathcal{S} = \mathcal{S}\,(\omega, k^2)$. However, from our photoproduction study [9], we know that in the threshold region, $M_{\pi^0} < \omega < 150$ MeV, the ω–dependence is mostly due to the unitarity cusp which is fixed by the Fermi–Watson final state theorem. Stated differently, this accounts for the dominant isospin breaking effect due to the sizeable pion mass difference, $\sqrt{(M_{\pi^+} - M_{\pi^0})/M_{\pi^0}} = 18\%$. We will discuss the numerical implications of this approximation later on. Consequently

$$\begin{aligned} E_{0+}(\omega, k^2) &= E(k^2) - \frac{e g_{\pi N} \omega_c^2}{32\pi^2 m F_\pi^2}\left(1 - \frac{5\omega_c}{2m}\right)\sqrt{1-y}\ , \\ L_{0+}(\omega, k^2) &= L(k^2) - \frac{e g_{\pi N} \omega_c^2}{32\pi^2 m F_\pi^2}\,\frac{1}{2+\rho}\left(1 - \frac{\omega_c}{2m}\,\frac{10 + 6\rho + \rho^2}{2+\rho}\right)\sqrt{1-y}\ , \end{aligned} \tag{32}$$

and the chiral expansion, Eq.(31), is applied to $\mathcal{S}(k^2)$. This means that we can calculate $\mathcal{S}(k^2)$ at threshold in the isospin limit. The Born terms are readily evaluated,

$$\begin{aligned} E(k^2)^{\rm Born} &= \frac{e g_{\pi N}}{8\pi m^2}\Big\{-M_\pi + \frac{1}{2m}[(3+\kappa_p)M_\pi^2 - (1+\kappa_p)k^2] \\ &\qquad + \frac{M_\pi}{8m^2}[(5+4\kappa_p)k^2 - 3(5+2\kappa_p)M_\pi^2]\Big\} \\ L(k^2)^{\rm Born} &= \frac{e g_{\pi N}}{8\pi m^2}\Big\{-M_\pi + \frac{3M_\pi^2 - k^2}{2m} + \frac{M_\pi}{8m^2}[(5-2\kappa_p)k^2 - 15M_\pi^2]\Big\}\ . \end{aligned} \tag{33}$$

The order q^3 one–loop contributions are given by

$$\begin{aligned} E(k^2)^{\rm q^3-loop} &= \frac{e g_{\pi N}\omega_c^2}{128\pi^2 m F_\pi^2}\left[\frac{\rho}{1+\rho} + \frac{(2+\rho)^2}{2(1+\rho)^{3/2}}\arccos\frac{-\rho}{2+\rho}\right]\ , \\ L(k^2)^{\rm q^3-loop} &= \frac{e g_{\pi N}\omega_c^2}{128\pi^2 m F_\pi^2}\left[\frac{2}{1+\rho} + \frac{\rho}{(1+\rho)^{3/2}}\arccos\frac{-\rho}{2+\rho}\right]\ . \end{aligned} \tag{34}$$

These are finite and can be checked against the result of the relativistic calculation presented in [5]. To get an idea about the uncertainties induced by

the approximation on the energy dependence discussed above, we have also evaluated to this order the full $\mathcal{S}(\omega, k^2)$. The difference of the full result and the approximation takes the form

$$\begin{aligned}
\Delta E_{0+}^{\mathrm{q}^3-\mathrm{loop}} &= \frac{e g_{\pi N} \omega_c^2}{128\pi^2 m F_\pi^3}\Big\{ \frac{\sqrt{y}}{y+\rho}\Big[\rho - (2y+3\rho)\sqrt{1-y} + \frac{4y+4\rho+\rho^2}{2\sqrt{y+\rho}} \\
&\quad \times H(y,\rho)\Big] - \frac{\rho}{1+\rho} - \frac{(2+\rho)^2}{2(1+\rho)^{3/2}}\,\arccos\frac{-\rho}{2+\rho} - 4\sqrt{1-y}\Big\}\ , \\
\Delta L_{0+}^{\mathrm{q}^3-\mathrm{loop}} &= \frac{e g_{\pi N} \omega_c^2}{128\pi^2 m F_\pi^3}\Big\{ \frac{y^{3/2}}{y+\rho}\Big[2 - 2\sqrt{1-y} + \frac{\rho}{\sqrt{y+\rho}}\,H(y,\rho)\Big] \\
&\quad - \frac{2}{1+\rho} - \frac{\rho}{(1+\rho)^{3/2}}\,\arccos\frac{-\rho}{2+\rho} + \frac{4}{2+\rho}\sqrt{1-y}\Big\}\ . \qquad (35)
\end{aligned}$$

We will come back to this later on. The order q^4 contributions to $\mathcal{S}(k^2)$ can be grouped into the graphs which are proportional to g_A and the ones proportional to g_A^3. These are no longer finite and depend on the scale of dimensional regularization, λ. The counter terms to be discussed below have an infinite piece to cancel these divergences and their scale–dependence is such that it cancels the one from the q^4 loops. The explicit form of these terms is (we first give the result of the g_A^3 graphs)

$$\begin{aligned}
E(k^2)^{\mathrm{ga}^3} &= \frac{e g_A^3 \omega_c^3}{128\pi^3 m F_\pi^3}\Big\{ (\frac{8}{3}+\frac{7\rho}{6})\frac{\ln}{\omega_c}\lambda - \frac{26}{9} - \frac{59\rho}{36} + \pi(\frac{5}{3}+\rho) \\
&\quad + (\frac{8}{3}+\frac{7\rho}{6})\sqrt{1+\frac{4}{\rho}}\,\ln\frac{\sqrt{4+\rho}+\sqrt{\rho}}{2} \qquad (36) \\
&\quad - 2(2+\rho)\int_0^1 dx \sqrt{1-x^2+\rho x(1-x)}\,\arccos\frac{x}{\sqrt{1+\rho x(1-x)}}\Big\}\ , \\
L(k^2)^{\mathrm{ga}^3} &= \frac{e g_A^3 \omega_c^3}{128\pi^3 m F_\pi^3}\Big\{ (\frac{2}{3}-\frac{5\rho}{6})\ln\frac{\omega_c}{\lambda} - \frac{8}{9} + \frac{13\rho}{36} + \pi(\frac{1}{6}-\frac{\rho}{2}) \\
&\quad + (\frac{5}{3}+\frac{\rho}{6})\sqrt{1+\frac{4}{\rho}}\,\ln\frac{\sqrt{4+\rho}+\sqrt{\rho}}{2} \\
&\quad + \int_0^1 dx \frac{4(1+\rho)x^2 + (\rho^2-2\rho-1)x - \rho(1+\rho)/2 - 2}{\sqrt{1-x^2+\rho x(1-x)}} \\
&\quad \times \arccos\frac{x}{\sqrt{1+\rho x(1-x)}}\Big\}\ , \qquad (37)
\end{aligned}$$

Similarly, one finds for the diagrams proportional to g_A (these form an independent subset of gauge invariant Feynman diagrams)

$$E(k^2)^{\rm ga} = \frac{e g_A \omega_c^3}{128\pi^3 m F_\pi^3}\Big\{(10+\frac{11\rho}{6})\ln\frac{\omega_c}{\lambda} - \frac{7}{3} - \frac{31\rho}{36} + (\frac{4}{3}+\frac{11\rho}{6})\sqrt{1+\frac{4}{\rho}}$$
$$\times \ln\frac{\sqrt{4+\rho}+\sqrt{\rho}}{2} - \frac{\pi\rho}{1+\rho} - \frac{\pi(2+\rho)^2}{2(1+\rho)^{3/2}}\arccos\frac{-\rho}{2+\rho} \qquad (38)$$
$$+\int_0^1 dx \frac{4(1+\rho)x^2-(4+6\rho)x-4}{\sqrt{1-x^2+\rho x(1-x)}}\arcsin\frac{x}{\sqrt{1+\rho x(1-x)}}\Big\}\ ,$$

$$L(k^2)^{\rm ga} - E(k^2)^{\rm ga} = \frac{e g_A \omega_c^3 (1+\rho)}{128\pi^3 m F_\pi^3}\Big\{-2\ln\frac{\omega_c}{\lambda} - 3$$
$$+\int_0^1 dx \frac{x(2x-1)}{1-x^2+\rho x(1-x)}\Big(-2-\rho+\frac{\pi(5+9\rho x/2-4(1+\rho)x^2)}{\sqrt{1-x^2+\rho x(1-x)}}$$
$$+\frac{2+(\rho-2)x-2(1+\rho)x^2}{\sqrt{1-x^2+\rho x(1-x)}}\arcsin\frac{x}{\sqrt{1+\rho x(1-x)}}\Big)\Big\}\ . \qquad (39)$$

Notice that the last integrand contains an integrable singularity of the type $1/\sqrt{1-x}$ for all $\rho > 0$. As a check, the last integral in Eq.(39) at $\rho = 0$ gives $\pi^2 - 3\pi + 9$. The one–loop corrections to order q^4 within the approximation on the energy–dependence are thus determined. Finally, we turn to the counter terms at this order. First, there are the two terms from $\mathcal{L}_{\pi N}^{(4)}$ which appeared already in the photoproduction case. We have refitted the sum $a_1 + a_2$ since in Refs.[9,10] the full ω–dependence of E_{0+} was considered. Within the same approximation used here, the value of $a_1 + a_2$ is 7.85 GeV^{-4} as compared to $a_1 + a_2 = 6.60$ GeV^{-4} from the full ω–dependence. We will also use this latter value as a measure for the theoretical uncertainty of our calculations. For the S–waves, we have a priori two new counter terms at order q^4,

$$E(k^2)^{\rm ct} = eM_\pi\{(a_1+a_2)M_\pi^2 - a_3 k^2\}\ ,$$
$$L(k^2)^{\rm ct} = eM_\pi\{(a_1+a_2)M_\pi^2 - a_3 k^2 + a_4(M_\pi^2 - k^2)\}\ , \qquad (40)$$

so that $L(k^2) - E(k^2) \sim (1+\rho)$. However, as proven in the appendix, in the soft pion limit one can show that

$$a_3 + a_4 = 0 \quad , \qquad (41)$$

and thus there is only one LEC and furthermore a strong correlation between $E(k^2)^{\rm ct}$ and $L(k^2)^{\rm ct}$ at order q^4. The low–energy constant a_3 will be treated as a free parameter and pinned down by a fit to the available differential cross section data at $k^2 = -0.1$ GeV^2. It turns out, however, that with a k^2–independent $L^{\rm ct}(k^2)$, i.e. with the k^2–dependence of $L(k^2)$ coming solely from the Born and loop graphs, one is not able to fit the existing data. We therefore have to include the first corrections to the soft–pion constraint Eq.(41) away

from the chiral limit. This induces terms of the type

$$E_{0+}^{\rm ct}, L_{0+}^{\rm ct} \sim a_5\, M_\pi^2\, k^2 \quad , \tag{42}$$

which are arising from terms in the Lagrangian $\mathcal{L}_{\pi N}^{(5)}$ and are thus of higher order. These are the minimal terms one has to take to be able to describe the data at $k^2 = -0.1$ GeV^2. Of course, there are other counter terms at this order. These, however, merely amount to quark mass renormalizations of the already considered k^2–independent counter terms and will therefore be set to zero here. In the next section, we show how to estimate the pertinent low–energy constants from resonance exchange. A fully consistent $\mathcal{O}(q^5)$ calculation would also include two–loop graphs and one loop graphs with insertions from $\mathcal{L}_{\pi N}^{(3)}$ (besides others). We take here the pragmatic approach and subsume all these effects in the effective couplings entering the higher order low–energy constants. In addition, the form factor correction due to the finite proton Dirac radius, cf. Eq.(13), contributes as follows,

$$E(k^2)^{\rm rad} = L(k^2)^{\rm rad} = -\frac{e g_{\pi N} M_\pi k^2}{48\pi m^2}\, \delta r_{1p}(\lambda) \ , \tag{43}$$

and is completely fixed from the knowledge of $< r^2 >_1^V$ [16], $\delta r_{1p}(\lambda = m) = 6.60 \pm 0.29$ GeV^{-2} using g_A as determined from the Goldberger–Treiman relation, $g_A = g_{\pi N} F_\pi / m = 1.328$. [6] This contribution is always treated separately. We now turn to the estimate of the size of the resonance contributions to the a_i $(i = 1, 2, 3, 4)$ and the P–wave low–energy constant b_P.

4 Resonance saturation of the low–energy constants

In this section, we consider the resonance saturation hypothesis to estimate the numerical values of the various low–energy constants. This principle works very well in the meson sector, see e.g. refs.[17–19] and is also a good tool to estimate the LECs in the presence of baryons, see e.g. [8] and [20]. In the baryon sector, resonance saturation proceeds in two steps. First, the effective field theory contains mesonic (M) and baryonic (N^*) excitations chirally coupled to the Goldstone bosons and the nucleons. Considering these excitations as very heavy, but keeping the ratios of coupling constants to masses fixed, one produces a string of higher dimensional operators involving only pions and nucleons with coefficients given in terms of the resonance parameters. Second,

[6] This value is not very different from the one in the relativistic calculation, $\delta r_{1p}^{\rm rel}(\lambda = 1\,{\rm GeV}) = 7.35$ GeV^{-2} [5].

one then performs the heavy mass expansion for the nucleons, i.e.

$$\tilde{\mathcal{L}}_{\rm eff}[U,M,N,N^*] \to \bar{\mathcal{L}}_{\rm eff}[U,N] \to \mathcal{L}_{\rm eff}[U,N_v] \ , \tag{44}$$

where N_v denotes the velocity–dependent heavy nucleon field (in general, we suppress the subscript 'v').

First, consider t–channel vector meson exchange, in this case the coupling of the ρ^0 and the ω to the nucleon and the subsequent vector meson decay into the $\pi^0\gamma^\star$ (a general discussion concerning the coupling of spin–1 fields to the pion–nucleon system has recently been given [21]). This leads to

$$\begin{aligned} a_1^V + a_2^V = a_3^V = -a_V^4 &= \frac{g_{\rho N}\,(1+\kappa_\rho)\,G_{\pi\rho\gamma}}{4\,\pi\,m\,M_\rho^2} + \frac{g_{\omega N}\,(1+\kappa_\omega)\,G_{\pi\omega\gamma}}{4\,\pi\,m\,M_\omega^2} \ , \\ b_P^V &= \frac{g_{\rho N}\,G_{\pi\rho\gamma}}{2\,\pi\,M_\rho^2} + \frac{g_{\omega N}\,G_{\pi\omega\gamma}}{2\,\pi\,M_\omega^2} \ , \end{aligned} \tag{45}$$

where the $V\pi^0\gamma$ couplings can be determined from the radiative widths $\Gamma(V \to \pi^0\gamma)$, $V = \rho^0, \omega$. The tensor to vector coupling ratio κ_V is known to be large for the ρ, $\kappa_\rho = 6 \ldots 6.6$, small for the ω, $\kappa_\omega = -0.16 \pm 0.01$. The ρN coupling constant is fairly well known whereas there is some sizeable uncertainty concerning $g_{\omega N}$. To avoid these uncertainties, we use a simpler form based in part on the gauged Wess–Zumino action, using the KSFR relation and setting $\kappa_\rho = 6$, $\kappa_\omega = 0$ (for details, see [9]),

$$a_1^V + a_2^V = a_3^V = -a_4^V = \frac{1}{16\pi^3 m F_\pi^3} \,, \quad b_P^V = \frac{5}{(4\pi F_\pi)^3} \ , \tag{46}$$

leading to $a_1^V + a_2^V = 2.67\,{\rm GeV}^{-4}$ and $b_P^V = 3.13\,{\rm GeV}^{-3}$ (see also [9]).

From the s–channel (baryonic) excitations, the dominant one is $\Delta(1232)$ exchange. We use the following $\Delta N\pi$ and $\Delta N\gamma$ Lagrangians

$$\begin{aligned} \mathcal{L}_{\Delta N\pi} &= \frac{3\sqrt{2} g_{\pi N}}{4m} \bar{\Delta}^\mu \Theta_{\mu\nu}(Z) \partial^\nu \vec{\pi} \cdot \vec{T}^\dagger N + {\rm h.c.} \\ \mathcal{L}_{\Delta N\gamma} &= \frac{i g_1}{2m} \bar{\Delta}^\mu \Theta_{\mu\lambda}(Y) \gamma_\nu \gamma_5 F^{\nu\lambda} T^{3\dagger} N \\ &\quad - \frac{g_2}{4m^2} \bar{\Delta}^\mu \Theta_{\mu\nu}(X) \gamma_5 F^{\nu\lambda} T^{3\dagger} \partial_\lambda N \\ &\quad - \frac{g_3}{4m^2} \bar{\Delta}^\mu \Theta_{\mu\nu}(X') \gamma_5 (\partial_\lambda F^{\nu\lambda}) T^{3\dagger} N + {\rm h.c.} \ , \end{aligned} \tag{47}$$

with

$$\Theta_{\mu\nu}(Z) = g_{\mu\nu} - (Z + \frac{1}{2})\gamma_\mu\gamma_\nu \quad . \tag{48}$$

N and Δ_μ denote the relativistic spin–1/2 (Dirac) and spin–3/2 (Rarita–Schwinger) field, respectively. The third term in $\mathcal{L}_{\Delta N\gamma}$ vanishes for real photons [22]. The off–shell parameters X, Y and Z are severely constrained from πN scattering, the nucleon polarizabilities and the fit to the new TAPS data for neutral pion photoproduction, for details see Ref.[10]. Using Eqs.(47), one finds for the Δ contribution to the a_i (to order q^4 in the Lagrangian)

$$\begin{aligned}
a_1^\Delta + a_2^\Delta &= \frac{g_{\pi N}\sqrt{2}}{24\pi m^3 m_\Delta^2}\Big\{ g_1\Big(\frac{m_\Delta^2 - m\,m_\Delta/2 - m^2}{m_\Delta - m} + mY(3-2Z) \\
&\qquad + m_\Delta(Y + Z + 4YZ)\Big) \\
&\quad + g_2\Big(\frac{3m}{8}(2X+1)(1-2Z) + \frac{m_\Delta}{4}(1 + X + Z + 4XZ)\Big)\Big\} \\
a_3^\Delta = -a_4^\Delta &= a_1^\Delta + a_2^\Delta + \frac{g_{\pi N}\sqrt{2}}{96\pi m^3 m_\Delta^2}\Big\{ m(2Z-1)[8g_1 Y + g_2(2X+1)] \\
&\quad + g_3[m(2X'+1)(2Z-1) - 2m_\Delta(1 + X' + Z + 4X'Z)]\Big\} \quad .
\end{aligned} \tag{49}$$

As discussed in the previous section, we have to account for the first correction to the soft–pion theorem $a_3 + a_4 = 0$. This is entirely given by Δ–exchange and contributes to L_{0+} as follows, [7]

$$L_{0+}^{\mathrm{ct},q^5} = -e\,M_\pi\,k^2\,(a_3 + a_4)^\Delta \quad , \tag{50}$$

with

$$\begin{aligned}
(a_3 + a_4)^\Delta &= \frac{g_{\pi N}\sqrt{2}M_\pi}{48\pi m^3 m_\Delta^2}\Big\{ g_1\Big[2Y(4Z-1) - \frac{m_\Delta}{m_\Delta - m}\Big] \\
&\quad + g_2\Big[\frac{X}{2}(4Z-1) + \frac{3m_\Delta^2 - 4m_\Delta m + 3m^2}{4m(m_\Delta - m)}\Big] \\
&\quad + g_3\Big[Z - X' - \frac{m_\Delta}{m}(1 + X' + Z + 4X'Z)\Big]\Big\} \quad ,
\end{aligned} \tag{51}$$

and similarly for E_{0+}

[7] We remark that this contribution to L_{0+} is the one which really gives the first correction to the soft-pion theorem whereas the equivalent E_{0+} term is a quark–mass renormalization of a_3.

$$
\begin{aligned}
a_3^\Delta = & \frac{g_{\pi N}\sqrt{2}M_\pi}{48\pi m^3 m_\Delta^2} \times \\
& \Big\{ g_1 \Big[-m^2(4YZ+4Y+Z+\frac{3}{2}) - m m_\Delta (8YZ-4Y+2Z+\frac{1}{2}) \\
& \quad + m_\Delta^2 (28YZ-4Y-7Z-7) - \frac{4m_\Delta^3}{m}(4YZ+Y+Z+1) \Big] \frac{1}{(m-m_\Delta)^2} \\
& + g_2 \Big[m(18YZ-7Y+9Z-\frac{7}{2}) - m_\Delta (30XZ-4X+12Z+\frac{1}{2}) \\
& \quad + \frac{m_\Delta^2}{m}(12XZ+3X+3Z+\frac{1}{2}) \Big] \frac{4}{m-m_\Delta} \\
& + g_3 \Big[-8X'Z-4Z+4X'+2+\frac{4m_\Delta}{m}(1+4X'Z+X'+Z) \Big] \Big\} \qquad (52)
\end{aligned}
$$

A good check on the lengthy expressions Eqs.(51,52) (together with the analogous terms of order M_π^4 not shown here) is that they fulfill the constraint $L(k^2) - E(k^2) \sim (1+\rho)$.

Furthermore, b_P^Δ is the same as in the photoproduction case [9],

$$
\begin{aligned}
b_P^\Delta = & \frac{g_{\pi N} g_1 \sqrt{2}}{12\pi m^2 m_\Delta^2} \Big\{ \frac{2m_\Delta^2 + m_\Delta m - m^2}{2(m_\Delta - m)} \\
& \quad + m(Y+Z+2YZ) + m_\Delta (Y+Z+4YZ) \Big\} \ . \qquad (53)
\end{aligned}
$$

The couplings g_1, g_2 and the off–shell parameter X, Y, Z have been previously determined from neutral pion photoproduction, πN scattering and the nucleons' electromagnetic polarizabilities. Nothing is known about the signs and magnitudes of g_3 and X'. These only show up in reactions with virtual photons. In what follows, we will use these two parameters to obtain a best fit to the MAMI and NIKHEF data at $k^2 = -0.1$ GeV^2. Since we do not constrain the magnitudes of g_3 and X', this effectively amounts to a free fit with $a_3 \neq a_4$. We finally remark that g_3 and X' also enter virtual Compton scattering and can eventually be pinned down within some broad ranges in the future.

5 Fit to the existing data

In this section, we show the combined fit to the NIKHEF ($\epsilon = 0.67$) [2] and the MAMI ($\epsilon = 0.582$ and 0.885) [3] data at $k^2 = -0.1$ GeV^2 and the resulting multipoles. Note that the MAMI data are ϕ–integrated differential cross sections involving only R_T and R_L. In Figs.2a,b, the dashed lines give the best fit at order q^4, i.e. with the soft–pion constraint $a_3 + a_4 = 0$. Clearly, this does not describe the data. If one adds, however, the order q^5 counter terms

for the S–wave multipoles as discussed in the previous sections, one finds an acceptable fit (solid lines) with a χ^2/dof of 2.296. In the resonance exchange picture, this amounts to

$$g_3 = -125.7 \pm 6.2 \ , \qquad X' = -0.22 \pm 0.09 \ . \tag{54}$$

Clearly, such a large value of the unknown third $N\Delta\gamma$ coupling constant indicates that one subsumes in its value other effects like e.g. from two–loop graphs. Alternatively, one can only take the q^4 counter terms and relax the constraint $a_3 = -a_4$ in the fit. This leads to $a_3 = -1.37$ GeV^{-4} and $a_4 = -0.22$ GeV^{-4}, which are numbers of natural size. We remark that in a combined fit to the NIKHEF and the MAMI data, it is not possible to correctly get the normalization of the two MAMI data sets for the two different values of the photon polarization ϵ, compare Fig.2b.

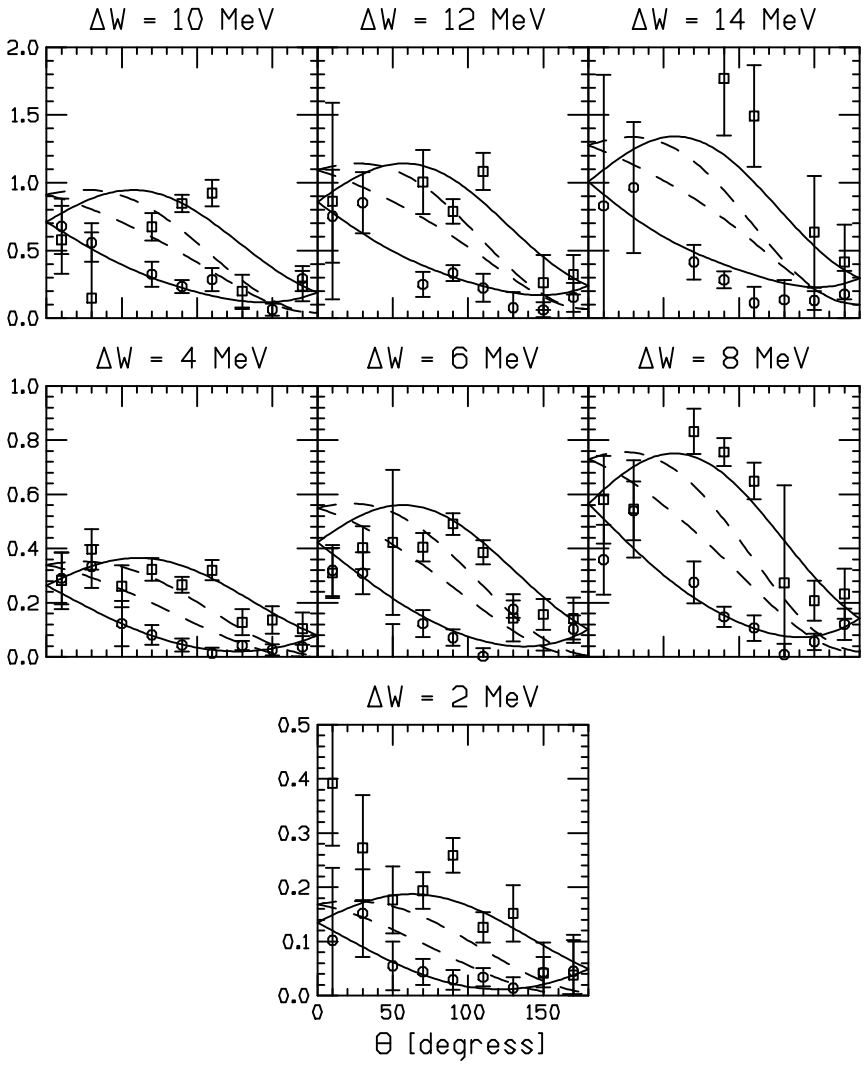

Fig. 2a: NIKHEF data. Open squares (circles): $\phi = 180^\circ$ (0°).

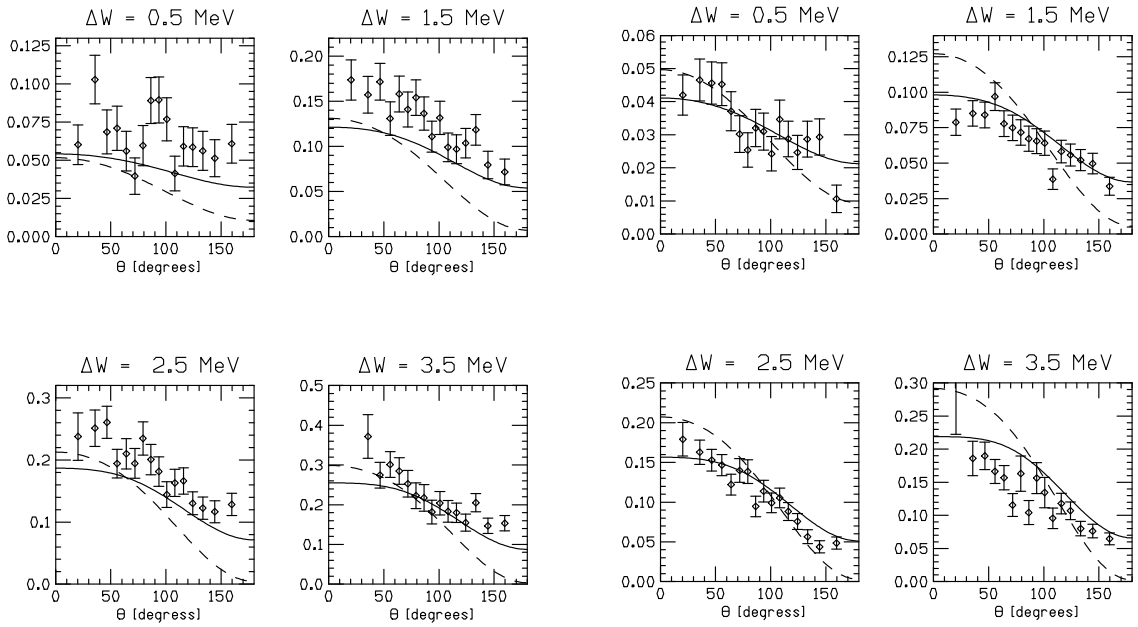

Fig. 2b: MAMI data. Left (right) panel: $\epsilon = 0.885\,(0.582)$.

The corresponding multipoles are shown in Fig.3 for $\Delta W = 0 \ldots 15$ MeV, all in units of $10^{-3}/M_{\pi^+}$. For the S–waves, we give the real and the imaginary parts, indicated by the solid and dashed lines, respectively. We remark that Re E_{0+} has changed sign as compared to the photoproduction case, it shows the typical cusp effect at the opening of the $\pi^+ n$ threshold. In contrast, Re L_{0+}

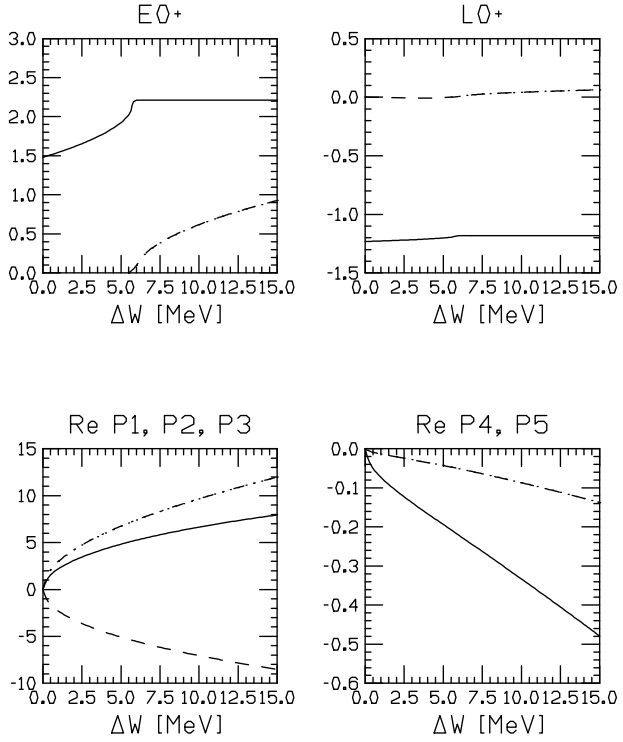

Fig. 3: Multipoles at $k^2 = -0.1$ GeV^2. See text for notations.

is essentially energy–independent with a very small cusp. For the P–waves, we only show the real parts since the imaginary parts are very small. The large P–waves are all of the same size as shown in the lower left panel (P_1, P_2, P_3: solid, dashed, dash–dotted line, in order) whereas P_4 and P_5 are more than one magnitude smaller, see the lower right panel in Fig.3 (P_4, P_5: solid and dashed line, respectively).

In Fig.4, we show the effect of the approximation on the ω–dependence. Without refitting any parameters, we have added the correction Eq.(34) to the S–wave multipoles. The solid curves in Fig.4 refer to the approximation and the dash–dotted ones to the complete ω–dependence in the loops to order q^3. We see that the effect on E_{0+} is small and somewhat more pronounced in L_{0+}. We remark that these curves should only be considered indicative since there is also a difference in the q^4–loops, which we did not evaluate in detail. Furthermore, part of this effect would be absorbed in the values of the LECs which we used in the fit.

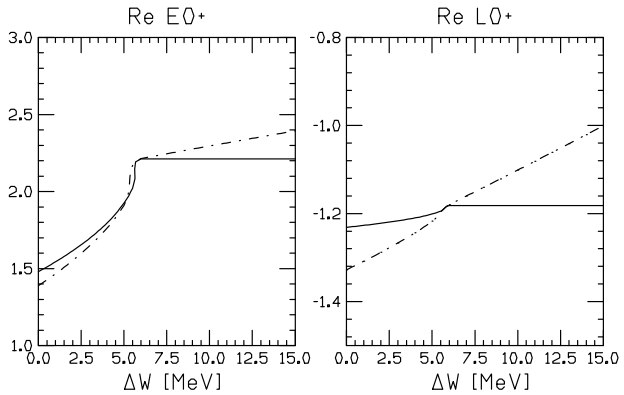

Fig. 4: Approximation on the ω–dependence at order q^3.

Furthermore, we have also performed some fits with the larger value of $b_p = 15.8$ GeV^{-3}. It leads to a somewhat larger (in magnitude) value of $g_3 = -145.8 \pm 6.2$ and $X' = -0.26 \pm 0.06$, consistent with the value given in Eq.(54). The χ^2/dof is 2.945, i.e. worse than for the smaller value of $b_p = 13.0$ GeV^{-3}. To improve the fits with the larger b_P, one thus would have to readjust the parameters in the photoproduction case. Clearly, this discrepancy deserves further experimental clarification. In what follows, we will always use the smaller value of b_p. We would like to stress again, see also [5], that for a good test of chiral dynamics, one needs data at lower photon virtualities as witnessed by the large value we find for the coupling constant g_3 and the necessity of using a particular dimension five operator. However, as $|k^2|$ decreases, the latter becomes less and less important. Finally, we note that the convergence in the S–wave loops and counter terms is slow, similar to the photoproduction case [9], whereas the Born terms at order q^5 can safely be neglected.

6 Predictions at lower photon virtualities

Having fixed all parameters at $k^2 = -0.1$ GeV^2, we can now make predictions for lower photon virtualities. We will concentrate here on the range of $|k^2|$ between 0.04 and 0.06 GeV^2 since at the upper end some data have been taken at MAMI and it is conceivable that in the near future one will not be able to go below 0.04 GeV^2 since the pion has to leave the target. [8]

In Figs. 5 and 6, we show the real parts of the S–wave and the large P–wave multipoles as a function of ΔW for $k^2 = -0.06, -0.05, -0.04$ GeV^2 (solid, dashed–dotted and dashed lines, in order). At threshold, Re E_{0+} passes zero for $k^2 \simeq -0.04$ GeV^2.

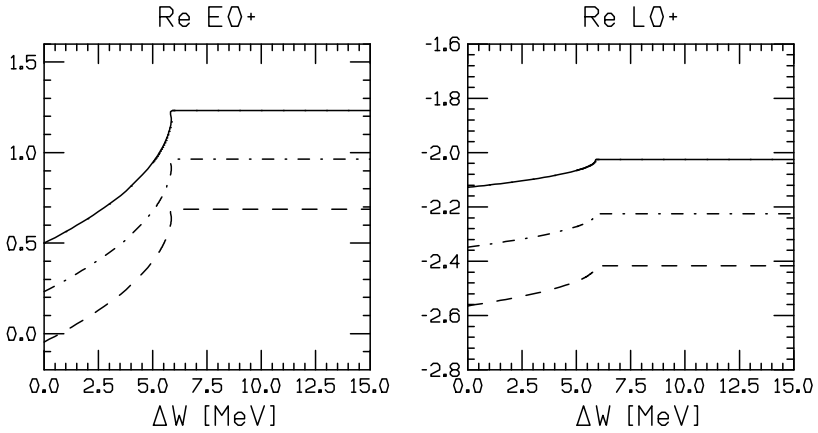

Fig. 5: Predictions for the S–wave mulitpoles. For notations, see text.

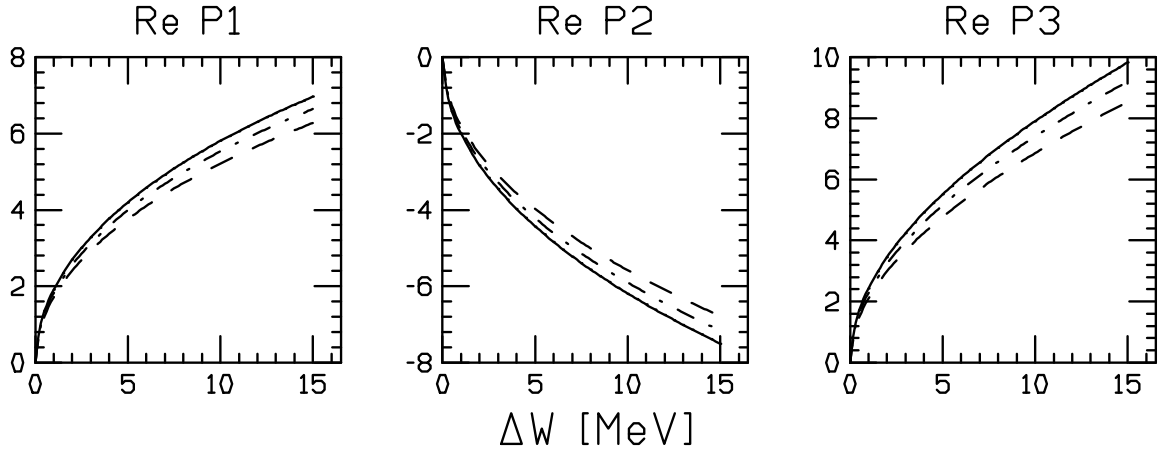

Fig. 6: Predictions for the P–wave mulitpoles. For notations, see text.

For the new MAMI data, we show the various differential cross sections at $k^2 = -0.06$ GeV^2 with $\epsilon = 0.582$ and $\Delta W = 2$ and 8 MeV as indicated by the

[8] Predictions at lower photon virtualities can be supplied upon request.

solid and dashed–dotted lines, respectively.

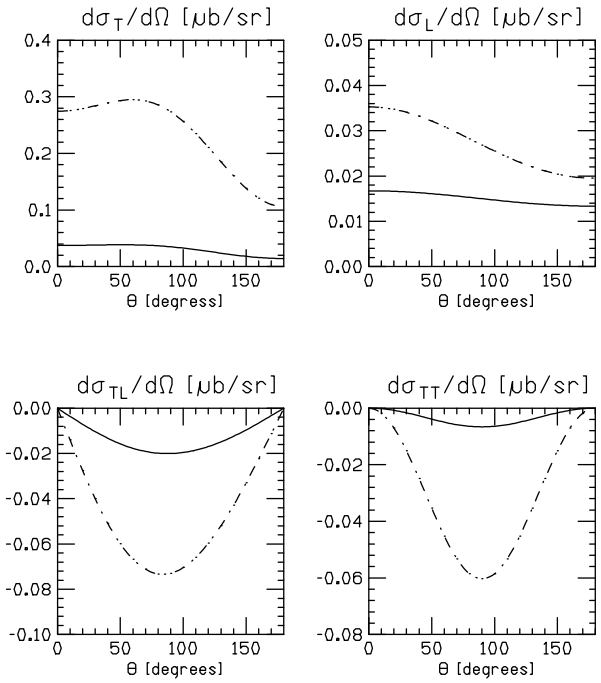

Fig. 7: Predictions for the differential cross sections. For notations, see text.

The S–wave cross section a_0, defined as

$$a_0 = |E_{0+}|^2 + \epsilon_L \, |L_{0+}|^2 \quad , \tag{55}$$

is shown in Fig.8. The data of Welch et al. [1] (open squares) are taken at different values of ϵ. This range is indicated by the dotted lines in Fig.8. The solid line refers to $\epsilon = 0.67$,

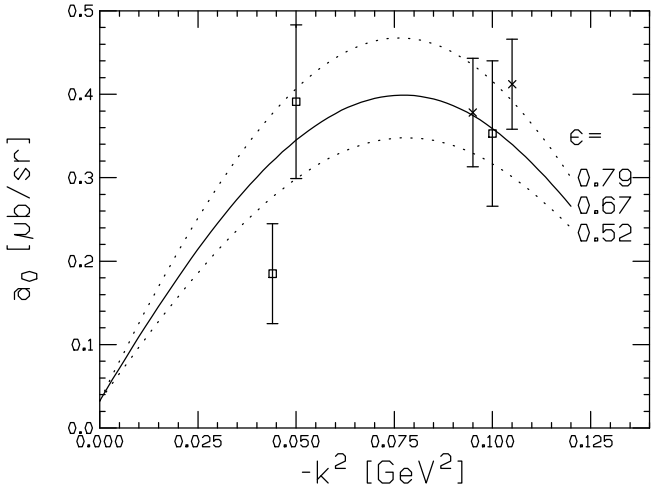

Fig. 8: S–wave cross section. For notations, see text.

i.e. the kinematics of van den Brink et al. [2] (crosses). Within the sizeable uncertainty, the S–wave cross section a_0 as predicted by the calculation is consistent with the data and shows again the flattening with increasing $|k^2|$ as already found in the relativistic calculation [23].

7 Summary and outlook

In this paper, we have considered neutral pion electroproduction off protons in the framework of heavy baryon chiral perturbation theory. The main results can be summarized as follows:

- Extending the successful photoproduction calculation [9] [10] to account for all k^2–dependent counter terms at order q^4 does not give a decent fit to the existing electroproduction data at the rather large $k^2 = -0.1$ GeV$^2 \simeq -5M_\pi^2$. This can be traced back to a particular soft–pion theorem which severely constrains the possible local dimension four contact terms. We are thus forced to take into account a particular dimension five operator which gives the first correction to the soft–pion theorem. With that term, the data can be fitted.
- We have given predictions for the $|k^2|$ range between 0.04 and 0.06 GeV^2, where new data have been and are going to be taken. At threshold, the real part of E_{0+} changes sign at $k^2 \simeq -0.04$ GeV^2. The calculated S–wave cross section is in satisfactory agreement with existing determinations. More detailed predictions pertaining to the relevant kinematics of future experiments are available from the authors.

Further improvements of the calculations presented here are:

- The P–wave multipoles should be calculated to one order higher. This would give a more accurate description of the small P–waves and can further be used to tighten the predictions of the P–wave LETs [15].
- The full–energy dependence of the loops should be taken into account when more accurate data will become available.
- A more systematic study of higher order effects than done here should be done to eventually pin down the $N\Delta\gamma$ parameters g_3 and X'.

Clearly, when more and more accurate data at lower photon virtualities will be available, neutral pion electroprodcution offers a variety of tests of the chiral QCD dynamics.

8 Acknowledgements

We are grateful to J.C. Bergstrom, A.M. Bernstein, H. Blok, M. Distler, D. Drechsel, O. Hanstein, L. Tiator, H.B. van den Brink and Th. Walcher for useful comments and communications.

A Counterterms at order q^4

Here, we wish to proof Eq.(41) which states that there are no polynomial S–wave counter terms with $a_3 + a_4 \neq 0$ up-to-and-including order q^4. For that, we follow appendix E of Ref.[5] and consider the soft–pion limit for the process $\gamma^\star(k) + p(p_1) \to \pi^0(q) + p(p_2)$, i.e. for $q_\mu \to 0$ (this includes the chiral limit $M_\pi \to 0$). In this limit, only the nucleon pole graphs (including the electromagnetic form factors and, in particular, the radius counter term) remain, for all values of the photon virtuality k^2. The corresponding non–pole amplitude (denoted by an 'overbar') must thus vanish,

$$\overline{J}_\mu = i\,\bar{u}_2\,\gamma_5\,\Big[\,\gamma_\mu\,\bar{B}_5 + 2P_\mu\,(\bar{B}_1 + \bar{B}_2 - m\bar{B}_6) + k_\mu\,(\bar{B}_1 + 2\bar{B}_4 - 2m\bar{B}_7)\Big]\,u_1 = 0 \tag{A.1}$$

where we use the notation of Ref.[5], i.e. $P = (p_1 + p_2)/2$ (see section 2 of that review). In the soft pion limit, the following conditions arise

$$\bar{B}_5 = 0 \quad \bar{A}_1 + \bar{B}_2 = 0\ , \quad \bar{B}_1 + 2\bar{B}_4 - 2m\bar{A}_6 = 0\ . \tag{A.2}$$

In fact, the $\bar{B}_5$, $\bar{B}_1 + 2\bar{B}_4$ and $\bar{A}_6$ are individually zero since they are odd under crossing, i.e. proportional to $(s-u) \sim q \cdot (p_1 + p_2)$.

Modulo irrelevant prefactors and setting $m = 1$, the S–wave multipoles are related to the invariant amplitudes A_i and B_i as follows (we drop the subscript '0+' and refer to [5] for definitions)

$$\begin{aligned} E &= \mu\bar{A}_1 + \mu^2\bar{A}_3 + \frac{\mu}{2}(\mu^2 - \nu)\bar{A}_4 - \nu\bar{A}_6 \\ L - E &= \frac{1}{2}(\mu^2 - \nu)[-\bar{A}_1 - \bar{B}_2 + \bar{B}_1 + 2\bar{B}_4 - \mu\bar{A}_4 - 2\bar{A}_6\,]\ , \end{aligned} \tag{A.3}$$

with $\nu \sim k^2 \sim \rho$ and $\mu \sim M_\pi$. To order q^4, the polynomial terms (in k^2) contributing to L, taking into account the crossing properties of the various

amplitudes, are solely given by $L = \mu\,\bar{A}_1 - \nu\,(\bar{B}_1 + 2\bar{B}_4)/2$, with

$$1)\;\; \bar{A}_1 = \alpha\, k^2 \;\;\text{and}\;\; 2)\;\; \bar{B}_1 + 2\bar{B}_4 = \beta\,(s-u)/2 = 2\,\beta\,\mu \;\; . \qquad \text{(A.4)}$$

Two cases are possible that could lead to $a_3 + a_4 \neq 0$, namely

$$i)\;\; \alpha \text{ or } \beta \neq 0 \;\; , \quad ii)\;\; \alpha \text{ and } \beta \neq 0 \text{ with } \alpha \neq \beta \;\; . \qquad \text{(A.5)}$$

However, gauge invariance ($\overline{J} \cdot k = 0$) (see Eq.(2.1) of Ref.[5]) implies that $\bar{B}_2 = -\beta\, k^2$. Furthermore, the second condition from Eqs.(A.2) leads to $\bar{B}_2 = -\alpha\, k^2$ (because of 1) in Eq.(A.4)). Clearly, α and β must be equal and both possibilities in Eq.(A.5) are ruled out. This gives the desired result, $a_3 + a_4 = 0$.

To summarize the argument, the soft pion theorem excludes a polynomial of the type $\bar{A}_1 = \text{const}\, k^2$ which would give rise to $a_3 + a_4 \neq 0$ for the non–pole contributions. Only the case $\bar{A}_1 = -\bar{B}_2 = \text{const}\, k^2\,,\;\; \bar{B}_{14} = \text{const}\,(s-u)/2$ is allowed leading immediately to the constraint. Evidently, this constraint does not apply to the nucleon pole graphs, compare Eq.(43).

References

[1] T.P. Welch et al., Phys. Rev. Lett. **69** (1992) 2761

[2] H.B. van den Brink et al., Phys. Rev. Lett. **74** (1995) 3561;
H.B. van den Brink, Thesis, Vrije Universiteit Amsterdam, 1995

[3] M. Distler, Thesis, University of Mainz, in preparation;
Th. Walcher, in "Chiral Dynmaics: Theory and Experiment", A.M. Bernstein and B.R. Holstein (eds), Springer Lecture Notes in Physics, Heidelberg, 1995;
Th. Walcher, plenary talk, "Baryons' 95", Santa Fe, USA, October 1995

[4] M. Distler and Th. Walcher, private communication

[5] V. Bernard, N. Kaiser, T.–S. H. Lee and Ulf-G. Meißner, Phys. Rep. **246** (1994) 315

[6] J. Gasser, M.E. Sainio and A. Švarc, Nucl. Phys. **B307** (1988) 779

[7] E. Jenkins and A.V. Manohar, Phys. Lett. **B255** (1991) 558

[8] V. Bernard, N. Kaiser and Ulf-G. Meißner, Int. J. Mod. Phys. **E4**, 193 (1995)

[9] V. Bernard, N. Kaiser and Ulf-G. Meißner,"Neutral Pion Photoproduction off Nucleons Revisited", Z. Phys. **C** (1995) in press

[10] V. Bernard, N. Kaiser and Ulf-G. Meißner, "Chiral Symmetry and the Reaction $\gamma p \to \pi^0 p$", Bonn and Strasbourg preprint CRN 95–38 and TK 95 30, 1995 [hep-ph/9512234]

[11] M. Fuchs et al., "Neutral Pion Photoproduction off the Proton Near Threshold", accepted for publication in Phys. Lett. **B**.

[12] J. Bergstrom et al., "Measurement of the ^{1}H(γ, π^0) cross section near threshold", Saskatoon preprint, December 1995.

[13] J. Bergstrom, Phys. Rev. **C52**, 1986 (1995)

[14] O. Hanstein, D. Drechsel and L. Tiator, private communication

[15] V. Bernard, N. Kaiser and Ulf-G. Meißner, Phys. Rev. Lett. **74** (1992) 3752

[16] P. Mergell, Ulf-G. Meißner and D. Drechsel, Nucl. Phys. **A596** (1996) 367

[17] G. Ecker, J. Gasser, A. Pich and E. de Rafael, Nucl. Phys. **B321** (1989) 311

[18] G. Ecker, J. Gasser, H. Leutwyler, A. Pich and E. de Rafael, Phys. Lett. **B223** (1989) 425

[19] J.F. Donoghue, C. Ramirez and G. Valencia, Phys. Rev. **D39** (1989) 1947

[20] Ulf-G. Meißner, in "Chiral Dynamics: Theory and Experiment", A.M. Bernstein and B.R. Holstein (eds.), Springer, Berlin, 1995

[21] B. Borasoy and Ulf-G. Meißner, "Chiral Lagrangians for Baryons coupled to massive Spin-1 Fields", Bonn preprint TK 95 31, 1995 [hep-ph/9511230]

[22] V. Pascaluta and O. Scholten, Nucl. Phys. **A591**, 658 (1995)

[23] V. Bernard, N. Kaiser, T.–S. H. Lee and Ulf-G. Meißner, Phys. Rev. Lett. **70** (1993) 387